Atmos. Chem. Phys. Discuss., 9, 9597–9645, 2009
www.atmos-chem-phys-discuss.net/9/9597/2009/

Atmospheric Chemistry and Physics Discussions

Parameterization of vertical diffusion and the atmospheric boundary layer height determination in the EMEP model

A. Jeričević[1], L. Kraljević[1], B. Grisogono[2], and H. Fagerli[3]

[1]Meteorological and Hydrological Service of Croatia, Zagreb, Croatia
[2]Andrija Mohorovičić Geophysical Institute, Department of Geophysics, Faculty of Science, University of Zagreb, Croatia
[3]Norwegian Meteorological Institute, Oslo, Norway

Received: 6 March 2009 – Accepted: 31 March 2009 – Published: 16 April 2009

Correspondence to: A. Jeričević (jericevic@cirus.dhz.hr)

Published by Copernicus Publications on behalf of the European Geosciences Union.

Abstract

A new vertical diffusion scheme, called Grisogono, has been implemented in the Unified EMEP (European Monitoring and Evaluation Programme) model. It is shown based on Large Eddy Simulation (LES) that the Grisogono method performs better than the operational O'Brien's polynomial, especially in the stable conditions. In this work, the operational and proposed new parameterization for eddy diffusivity *K(z)* have been validated against observed daily surface nitrogen dioxide (NO_2), sulphur dioxide (SO_2) and sulphate (SO_4^{-2}) concentrations at different EMEP stations during year 2001. Moderate improvement in the correlation coefficient and bias for NO_2 and SO_2 and slight improvement for sulphate is found for most of the analyzed stations with the Grisogono *K(z)* scheme, which is recommended for further application due to its scientific and technical advantages. Special emphasis is given to the representation of the atmospheric boundary layer (ABL) in order to capture vertical transport and dispersion of atmospheric air pollution. Two different ABL schemes are evaluated against radiosounding data in January and July 2001, and against data from the Cabauw tower, the Netherlands, in the same year. Based on validation of the ABL parameterizations, it is found that the EMEP model is able to reproduce spatial and temporal mixing height variability. Improvements are identified especially in stable conditions with the new ABL scheme based on the bulk Richardson number (Ri_B).

1 Introduction

Air quality models are nowadays recognized as an important tool for air quality assessment. Although measurements are the basis of air quality assessment, there are several advantages provided by models: high spatial and temporal resolution of simulated data, forecasting of the air quality as a result of changes in emissions or/and meteorological conditions and a better understanding of the physical processes that drive the transport of pollutants in the atmosphere. For nearly 30 years, the European

Monitoring and Evaluation Programme (EMEP) under the Convention on Long-Range Transboundary Air Pollution (LRTAP), has been responsible for development of air quality modelling systems to support the design of environmental control strategies in Europe. The Unified EMEP model was developed and used to simulate transboundary transport of air pollution on European scale. Recently, special applications of the model have been developed at higher resolutions, and coupled with different meteorological drivers: EMEP4UK (e.g. Vieno et al., 2009a, b) and EMEP4HR (Jeričević et al., 2007; Kraljević et al., 2008). Development of the EMEP model includes detailed meteorological effects that become progressively more important on the finer spatial scale, such as turbulence and convection generated by a complex terrain. As a first step of the EMEP model development on a finer horizontal scale, turbulence parameterizations; particularly vertical diffusion scheme *K(z)*; needs to be tested.

In previous studies it has already been shown that parameterizations of *K(z)* have significant impacts on simulated chemical concentrations (e.g. Nowacki et al., 1996; Biswas and Rao, 2000; Olivie et al., 2004). Different parameterizations for *K(z)*, depending on stability in the atmospheric boundary layer (ABL), have been proposed (e.g. O'Brien, 1970; Deardorf, 1972; Louis, 1979; Holtslag and Moeng, 1991; Holtslag and Boville, 1993; Grisogono, 1995). O'Brien (1970) suggested a simple parameterization *K(z)* scheme used in many air quality models ranging from simple 1-D models (e.g. Lee and Larsen, 1997) towards application as in complex chemical models e.g. Comprehensive Air Quality Model with Extensions (CAMx, http://www.camx.com/; ENVIRON, 1998; Zhang et al., 2004), as well as in the EMEP model (Fagerli and Eliassen, 2002). In CAMx there are few *K(z)* parameterization schemes, with the O'Brien scheme as one of the options. Presently, in the EMEP the O'Brien scheme is used for the convective boundary layer (CBL), while in the stable boundary layer (SBL) conditions *K(z)* based on Monin – Obukhov (M-O; Monin and Obukhov, 1954) similarity theory is applied. There are many studies which show that the surface-layer formulations based on the M-O theory are often not applicable in the statically stable conditions (e.g. Mahrt, 1999; Pahlow et al., 2001; Poulos and Burns, 2003; Mauritsen et al., 2007; Grisogono et al., 2007). A new proposed scheme, called Grisogono, is implemented in the model and it is not based on the M-O similarity theory. The Grisogono scheme uses a linear-exponentially decaying profile, generalizing the O'Brien third-order polynomial *K(z)* (Grisogono and Oerlemans, 2001 and 2002). It has already been shown, based on Large Eddy Simulation (LES) and experimental data sets that the Grisogono method performs better than the O'Brien's polynomial, especially in the stable conditions (Jeričević and Večenaj, 2009a).

Special emphasis is given on the ability of the ABL scheme to capture vertical transport and dispersion of the atmospheric air pollution. Significant influence of the ABL height (H) on surface nitrogen oxide (NO_x) and particulate matter (PM) concentrations is found in urban and suburban areas e.g. Schafer et al. (2006), while Athanassiadis et al. (2002) show that an accurate H determination is needed to properly simulate pollutant levels with the grid-based photochemical models. Furthermore, H is explicitly included in the both EMEP *K(z)* parameterizations therefore it is important to evaluate EMEP model ability to simulate spatial and temporal variability of H. The operational (e.g. Jakobsen et al., 1995; Seibert et al., 2000) and the new ABL scheme based on the bulk Richardson number (Ri_B) are evaluated. The Ri_B method is the standard and widely used approach to derive H from numerical weather prediction (NWP) models, as well as from radiosounding data (e.g. Mahrt, 1981; Troen and Mahrt, 1986; Sørensen et al., 1996; Fay et al., 1997; Seibert et al., 2000; Zilitinkevich and Calanca, 2000; Zilitinkevich and Baklanov, 2002; Gryning and Batchvarova, 2002; Jeričević and Grisogono, 2006).

In this work, prior to application in the EMEP model, evaluation of the *K(z)* schemes on LES data is provided. Following, operational version of the EMEP model, and version with new parameterization schemes (i.e. *K(z)* and ABL schemes) are verified by comparing one full year of modelled data against the corresponding set of measurements from different EMEP stations in Europe. Based on that validation, uncertainties (both in the measurements and in the model) are established. Pronounced differences between performances of the two model versions and impacts on simulated concentrations are investigated and recommendations for future work are provided. This paper gives the basis for further development and improvement of the EMEP model by e.g. improving parameterizations of the vertical diffusion and the boundary layer representation. This study has been conducted within the EMEP4HR project which main purpose is to develop and test an operative framework for environmental control of air pollution problems in a broader region of Croatia. Previous efforts addressing to the same issue are described in Klaić (1990, 1995) and Beširević (1998).

2 Methods

2.1 The EMEP model description

The Unified EMEP model (http://www.emep.int/) was developed at the Norwegian Meteorological Institute under the EMEP programme. The Unified EMEP model is a development of earlier EMEP models (Berge and Jakobsen, 1998 and Jonson et al., 1998, and fully documented in Simpson et al., 2003 and Fagerli et al., 2004). The model has been extensively validated against measurements (Fagerli et al., 2003, 2007; Simpson et al., 2006a, b, 2007; Jonson et al., 2006; Tsyro et al., 2007; Fagerli and Aas, 2008). It simulates atmospheric transport and deposition of acidifying and eutrophying compounds, as well as photo-oxidants and particulate matter over Europe. The model domain covers Europe and the Atlantic Ocean with the grid size 50 km×50 km while in the vertical there are a 20 terrain influenced layers reaching up to 100 hPa. The Unified EMEP models uses 3-hourly meteorological data from PARallel Limited Area Model with Polar Stereographic map projection (PARLAM-PS), which is a dedicated version of the HIgh Resolution Limited Area Model (HIRLAM) model for use within the EMEP. In this work the Unified EMEP model version rv2_6_1 was used.

ACPD

9, 9597–9645, 2009

Parameterization of vertical diffusion

A. Jeričević et al.

2.2 LES data

In this work data from DATABASE64 (Esau and Zilitinkevich, 2006) have been used in order to illustrate performance of two different *K(z)* schemes in stable atmospheric conditions. Full comprehensive evaluation of numerous LES runs have been provided in Jeričević and Večenaj (2009) including a wide range of neutral and stably stratified cases.

2.3 Measurements

Different data sets have been used here to evaluate EMEP model performance: (i) observed daily surface concentrations of NO_2, SO_2 and SO_4^{-2} at different EMEP stations in Europe during year 2001 (Fig. 1), (ii) radiosounding measurements from various European cities in January and July 2001 (Table 1) and (iii) wind and temperature profiles from the Cabauw tower, the Netherlands, also in year 2001.

The selected pollutants are the most important acidifying and eutrophying pollutants contributing to the air pollution. Furthermore, oxides of nitrogen are among the most important molecules in the atmospheric chemistry, while SO_2 is a predominant anthropogenic sulphur-containing air pollutant. Sulphate is a secondary pollutant, oxidant of SO_2, which is contributing to acid rain formation. Since atmospheric lifetimes of SO_2, NO_2 are 1 to 3 days and their oxidation products lifetime is generally even longer (Seinfeld and Pandis, 1998) they are subjected to the atmospheric transport and mixing processes, and therefore suitable for validation of vertical diffusion scheme efficiency. Furthermore, NO_2, SO_2 and SO_4^{-2} are monitored on the majority of EMEP stations providing a good spatial and time resolution of observations.

2.3.1 Measurements from the EMEP stations

For the particular purpose of model evaluation in this study measurements at the EMEP stations (http://www.emep.int/) have been used. They are well documented, quality controlled and they mostly represent background conditions over a larger area. In order to obtain data that are characteristic for long-range transport, it is important that station is representative of the EMEP 50×50 km^2 grid square averages. It should be emphasised that the recommendation for the EMEP site not to be influenced by local pollution implies that their location is chosen to ensure representativeness of the minimum concentration in the grid, not the grid average. Also measurements are not of equal quality on all stations and to some extent it may be explained by different measurement method (e.g. Fagerli et al., 2003).

Analyzed stations within the EMEP domain are shown in Fig. 1. Most of the stations are below 300 m (blue dots). Nevertheless, many stations in the Central European area are located between 600 m and 1000 m, while in the Alps area stations are often above 1000 m. Note that the station of Jungfraujoch (CH01) in Switzerland is above 3000 m and Chopok (SK02) in Slovakia is above 2000 m. Mountain stations are not very well represented in models with the coarse horizontal resolution, having too low altitude in the model and consequently surface concentrations are too high compared to measurements. The orography misrepresentation is a known modelling problem (e.g. Žagar and Rakovec, 1999; Ivatek Šahdan and Tudor, 2004) which is a result of orography averaging due to insufficient horizontal resolution in models.

List of all EMEP stations with more details about measuring programme and available data can be found at: http://tarantula.nilu.no/projects/ccc/network/index.html. Number of used stations varied from element to element i.e. the measured daily SO_2 was available at 68 stations, NO_2 at 43 stations and SO_4^{-2} at 58 stations.

2.3.2 Measurements from the radiosounding stations

Radiosoundings are often used in order to operationally determine and verify H values (e.g. Seibert et al., 2000). Nevertheless, these measurements are usually only taken twice a day at 00:00 and 12:00 UTC and consequently, the soundings can only be used as an overall reference. The data posses reasonably good spatial distribution over Europe and they are commonly available and quality controlled. In this work, the evaluation was performed using data obtained from 24 different measuring stations in Europe (Table 1) during January and July in 2001.

2.3.3 Cabauw measurements

Cabauw tower is located in the western part of the Netherlands (51°58′ N, 4°56′ E) with the flat surroundings e.g. van Ulden and Wieringa (1995). Temperature and wind averages are computed over 10-min intervals. Wind speed and wind direction are measured at six levels: 10, 20, 40, 80, 140 and 200 m while temperature is measured at one additional level, i.e. on 1.5 m. Pressure is measured at 1.5 m height only. In order to derive potential temperature needed for the Ri_B, hydrostatic balance is assumed. Pressure on upper levels is integrated from the surface pressure at 1.5 m using the trapezoidal rule. The Cabauw observations have been used in other studies to validate land surface parameterization schemes e.g. Beljaars and Bosveld (1997), Chen et al. (1997) and Ek and Holtslag (2005).

Measurements from the Cabauw tower have a high resolution in time and their vertical distribution is dense enough to reconstruct physical processes in the surface layer (occasionally even higher) thus providing the possibility to investigate and analyze the ABL structure near the surface in more details than with "standard" measurements.

2.4 Description of *K(z)* parameterization schemes

In the EMEP model *K(z)* is initially calculated from the surface to the top of the domain with the local scheme proposed by Blackadar (1979):

$$K(z) = K_{\min} + 1.1\frac{Ri_C - R_i}{Ri_C} l^2 \left|\frac{\partial \vec{V}}{\partial z}\right|, \tag{1}$$

where l is a mixing length and $K_{\min}$ is the background value $0.001\,\mathrm{m^2\,s^{-1}}$, $\left|\frac{\partial \vec{V}}{\partial z}\right|$ is the absolute value of wind shear in the vertical, R_i is the gradient Richardson number defined as:

$$Ri = \frac{g\partial\theta_v/\partial z}{\theta_v(\partial\vec{\mathbf{V}}/\partial z)^2} \tag{2}$$

where θ_v is a virtual potential temperature, and Ri_C is the critical Richardson number calculated from McNider and Pielke (1981) equation:

$$Ri_C = A\,(\Delta z)^B\,, \tag{3}$$

where A=0.115, B=0.175 and Δz is the model layer thickness. Final Ri_C value is: Ri_C=MAX$\left(0.25, 0.115(\Delta z)^{0.175}\right)$, obviously with the $\Delta z\rightarrow 0$ the $Ri_C\rightarrow 0.25$.

In the unstable ABL, *K(z)* is recalculated with the O'Brien scheme:

$$K(z) = K_H + \left[(z-H)^2/(\Delta z)^2\right] \times \tag{4}$$

$$\left\{K_{H_S} - K_H + (z - H_S)\left[\partial K_{H_S}/\partial z + 2(K_{H_S} - K_H)/\Delta z\right]\right\}$$

where K_H is a *K(z)* value at the top of the ABL, i.e. $K(z{=}H)$ and K_{H_S} is a *K(z)* value at the top of the surface-layer (H_S). It is assumed that $\partial K_H/\partial z$=0, and $\Delta z = H - H_S$. From the M-O similarity theory for the surface layer (e.g. Stull, 1988):

$$K_{H_s} = \frac{u_* \cdot k \cdot H_s}{\Phi\left(\frac{z}{L}\right)} \tag{5}$$

where k is the von Karman constant, $k\approx 0.41$, u_* is a frictional velocity and Φ is an universal function. Universal functions Φ used in the EMEP are those recommended by Garratt (1992) in unstable case:

$$\Phi = \left(1 - 16\frac{z}{L}\right)^{-1/2}, \tag{6a}$$

and in stable case:

$$\Phi = 1 + 5\frac{z}{L} \tag{6b}$$

The Obukhov length (L), is given by the near-surface turbulent fluxes of momentum,τ, and heat, Q_h, which are taken from the NWP PARLAM-PS model:

$$L = \frac{\theta_S \cdot u_*^2}{k \cdot g \cdot \theta_*}, \tag{7}$$

$$-u_* \theta_* = \frac{Q_h}{C_p \rho}, \tag{8}$$

$$\frac{\tau}{\rho} = u_*^2, \tag{9}$$

where θ_S is a surface potential temperature, θ_* is a potential temperature scale, g is acceleration of gravity, C_p is a specific heat capacity at constant pressure and ρ is air density.

The new proposed scheme is a linear-exponential method where the O'Brien third-order polynomial *K(z)* is generalized into a linear-exponential function (Grisogono and Oerlemans, 2002):

$$K(z) = (K_{\max} e^{1/2}/h) z \exp\left[-0.5(z/h)^2\right], \tag{10}$$

where h is the height of $K_{\max}$. Comparing the O'Brien, Eq. (4), and the Grisogono, Eq. (10), one can notice that one of the advantages of Eq. (10) in respect to Eq. (4) is that it needs only two input parameters, $K_{\max}$ and h. Those parameters are evaluated from the following equations:

$$K_{\max} = C(K) H u_* \tag{11}$$

$$h = H/C(h) \tag{12}$$

where $C(K)$=0.1 and $C(h)$=3 are empirical constants, estimated based on the LES data (Jeričević and Večenaj, 2009a). Both methods, the O'Brien and Grisogono, are non-local approaches and mainly depend on position and intensity of $K_{\max}$. In the Grisogono approach value of $K_{\max}$ explicitly includes u_* and H, utilized from the meteorological driver and its accuracy is constrained with the NWP model performance. On the other hand the O'Brien scheme represents *K(z)* as a polynomial function that depends on parameters:K_H, K_{H_S}, H, H_S. Note that these parameters e.g. H_S are not easy to resolve and describe especially in statically stable conditions (e.g. Zilitinkevich and Calanca, 2000; Jeričević and Grisogono, 2006; Mahrt, 2007).

2.5 Description of methods for the ABL calculation

Boundary layer height is an important parameter, which limits the modelled vertical extent of turbulent mixing in the atmosphere starting from the surface. The operational method for the calculation of H in the EMEP model determines H from the NWP PARLAM-PS output (Jakobsen et al., 1995). In stable conditions H is calculated as the height where $K(z)<1\,\mathrm{m}^2\,\mathrm{s}^{-1}$, with *K(z)* profiles calculated with the local Blackadar method Eq. (1) and vertically linearly smoothed over few adjacent layers. In unstable conditions hourly Q_h is distributed vertically via dry adiabatic adjustment and H is the height of the corresponding adiabatic layer. Finally, H is determined from:$H=\mathrm{MAX}(H_{\mathrm{stable}}, H_{\mathrm{unstable}})$.

The proposed Ri_B method is based on the assumption that continuous turbulence vanishes beyond Ri_{BC}, some previously defined critical value of Ri_B. The height at which Ri_B reaches Ri_{BC}, is considered as H. It is defined as:

$$Ri_B = \frac{g(z_j - z_1)}{\overline{\theta}} \frac{\theta_j - \theta_1}{(\Delta u_j)^2 + (\Delta v_j)^2}, \qquad j = 2, \ldots, 20 \text{ are the model levels.} \tag{13}$$

$$(\Delta u_j)^2 = (u_j - u_s)^2 = (u_j - 0)^2 = u_j^2 \tag{14}$$

$$(\Delta v_j)^2 = (v_j - v_s)^2 = (v_j - 0)^2 = v_j^2 \tag{15}$$

Here θ_1 is the potential temperature at the lowest model level, z_1, and $\bar{\theta}$ is the average potential temperature between levels 1 and j, H is the height of the level where Ri_{BC} is reached, and Ri_{BC}=0.25 was used. However, the supposed existence of Ri_{BC} recently receives criticism (Zilitinkevich and Baklanov, 2002; Jeričević and Grisogono, 2006; Mauritsen et al., 2007; Zilitinkevich et al., 2008; Grisogono and Belušić, 2008) and development of higher order *K(z)* schemes is a subject of current and future research. Main advantages of this method over the operational approach are that Ri_B includes two major turbulence generators in the atmosphere: thermal and mechanical sources of turbulence, represents an integral atmospheric properties and it is applicable in stable and unstable conditions. The Eq. 13 describes the H as an integral property that relates surface processes to upper processes in the ABL and thus embeds non-local effects. The main weakness of the operational ABL method in stable conditions is dependence on vertically integrated *K(z)* calculated with the Blackadar approach (Eq. 1). In unstable conditions its accuracy depends on surface parameters from the NWP model e.g. Q_h and vertical distribution via dry adiabatic adjustment while effects of the mean wind shear is not included.

3 Results

3.1 *K(z)* evaluation based on LES data

Prior to incorporation of a new turbulence parameterization schemes into a complex chemical model it is recommended to make an evaluation based on measurements and/or LES data. In Fig. 2 vertical profiles of mechanical eddy diffusivity, K_m, calculated with the O'Brien (Eq. 4), and the Grisogono (Eq. 10) scheme applied at the LES data are represented. Two stability classes from the numerous LES simulations were used: nocturnal (Fig. 2a) and long lived stable class (Fig. 2b). Nocturnal boundary layers develop in a neutral atmosphere while heat is lost at the surface. These boundary layers occur during night-time over land with near-neutral residual layer from daytime convective boundary layer and the surface is radioactively cooling. Case with stronger stability, i.e. long-lived stable class, has surface cooling with background stratification. It can be found at high latitudes over land during wintertime. In both stable cases better agreement of the Grisogono scheme is evident, while O'Brien underestimated the LES data. The unstable conditions were not simulated in the LES, however both schemes were incorporated in the EMEP model and evaluated during July 2001 against observed surface NO_2 concentrations and lower underestimation, i.e. higher surface concentrations, was found with the Grisogono scheme. More evaluation results can be found in Jeričević and Večenaj (2009).

3.2 Evaluation of the operational EMEP model performance in year 2001

The r and $\mathrm{BIAS}=\left(\frac{\mathrm{Model}-\mathrm{Observation}}{\mathrm{Observation}}\right)\times 100\%$ are calculated between the observed daily surface NO_2, SO_2 and SO_4^{-2} concentrations ($c(NO_2)$, $c(SO_2)$, $c(SO_4^{-2})$), and the corresponding modelled values calculated with the operational model set-up in year 2001 for different EMEP stations (Fig. 1). Evaluation show a good agreement with measurements and correlation coefficient $0.5 \leq r\ (NO_2) \leq 0.75$ is found on 56% stations, $0.5 \leq r(SO_2) \leq 0.77$ is on 43% stations, and $0.5 \leq r\ (SO_4^{-2}) \leq 0.87$ is on 86% stations. It should be pointed out that $r(SO_4^{-2})$ is the highest among all analyzed species with $r(SO_4^{-2})>0.7$ on 31% stations. Based on one year of data it is found that model underestimates measured $c(NO_2)$ with $\mathrm{BIAS}(NO_2) \approx -20\%$. For the SO_2 generally an overestimation is found with the EMEP model on 71% stations with $\mathrm{BIAS}(SO_2) \approx 30\%$, while model generally underestimates sulphate with $\mathrm{BIAS}(SO_4^{-2}) \approx -12\%$. Overestimation of SO_2 and underestimation of sulphate indicates that transformation processes should be intensified or precipitation and moisture are under predicted in the NWP model. The analyzed year was not exceptional regarding meteorological conditions and the EMEP model performance is in agreement with previous evaluation results (Fagerli et al., 2003).

3.3 Uncertainty in the measurements

Based on the operational EMEP model evaluation in year 2001, uncertainties in the measurements are identified. Discrepancies, with factor of 2 or more, between the model measurements are appointed on different stations which can be categorized as: (i) stations where peak events or episodes occurred in measurements influenced by local emission sources, and stations in the vicinity of large emission sources (shipping area in the North Sea) and (ii) mountain stations.

Changes in r and BIAS values, obtained by varying two different *K(z)* schemes in the model, are analyzed at all available stations in the EMEP domain (Figs. 6, 7, 8 and 9). Stations with the highest uncertainties were excluded from yearly r and BIAS estimation (Fig. 10).

3.3.1 Episodes

Underestimation of NO_2 with BIAS$<-30\%$, is found at some stations in Ireland, Switzerland, Poland and Italy (not shown). For example, Payerne (CH02) in Switzerland is located near the motorway, and therefore the corresponding measured $c(NO_2)$ had significantly higher values than the other EMEP stations in that region. An overestimation of NO_2 is found for Scandinavian stations, NO01, SE02 and DK08 located at the entrance to the Baltic Sea, where emissions from the shipping in the model are significant. In the EMEP summary report by Fagerli et al. (2003) the NO_2 time series from year 1990 to 2000 have been analyzed and a decrease in observations for station SE02 is evident with an annual average $\bar{c}(NO_2)_{1990}$=2.19 μg(N)m^{-3} in year 1990 toward $\bar{c}(NO_2)_{2000}$=1.51 μg(N)m^{-3} in year 2000. Corresponding modelled values are $\bar{c}(NO_2)_{1990}$=2.89 μg(N)m^{-3}, and $\bar{c}(NO_2)_{2000}$=2.45 μg(N)m^{-3}. Annual emissions of nitrogen oxides in the period 1996–2000 were mainly decreasing in the shipping area of Baltic countries (e.g. Bartnicki et al., 2002) which is reflected on the modelled annual concentrations. While in year 2001 observed annual average continued to decrease $\bar{c}(NO_2)_{2001}$=1.47 μg(N)m^{-3}, in the model $\bar{c}(NO_2)_{2001}$=3.68 μg(N)m $^{-3}$ with the

O'Brien, and $\bar{c}(NO_2)_{2001}$=4.60 μg(N)m $^{-3}$ with the Grisogono method. Obviously more stable conditions were simulated than it was observed, and since Grisogono method was less diffusive than O'Brien in stable conditions, average daily surface concentrations were higher with the Grisogono approach. Few other stations in the shipping area also had notably high BIAS for SO_2, those are: DK03, DK05, DK08, EE11, IE02, GB07 and SE02. On the other hand results with the Community Multiscale Air Quality (CMAQ, http://www.cmaq-model.org/, Matthias et al., 2007) model, with 18 km×18 km grid nested in 54 km×54 km horizontal grid, exhibit underestimation of $c(NO_2)$ at the same station SE02 for January and July 2001. Generally, stations in the North Sea shipping area are probably overestimated with the EMEP model due to coarse model horizontal resolution but it might be due to other reasons e.g. emissions, meteorology, chemistry, etc.

In Fig. 3 annual time series of the observed and modelled $c(NO_2)$ during year 2001 are represented for two selected stations: a) Westerland/Wenningstedt (DE01) with r>0.7 and b) Svratouch (CZ01) with r≈0.1. Although the agreement between the modelled and the observed $c(NO_2)$ in other periods was good, the summer peaks at e.g. CZ01 were not captured by the model which led to lower values of r. Note that both applied *K(z)* schemes had similar performance during the peak events.

Further, during the year peaks in $c(SO_2)$ and $c(SO_4^{-2})$ were also observed that were not captured in the model. In Fig. 4 time series of $c(SO_2)$ in year 2001 are shown for two selected stations: a) Ilmitz (AT02) with r>0.75 and b) Vorhegg (AT05) with r=0.25. Lower r at AT05 is likely a consequence of discrepancies between the model and the observations during peaks events. For SO_4^{-2} only few stations have lower r values also with stronger local influence. Time series of $c(SO_4^{-2})$ are shown in Fig. 5 for a) Neuglobsow (DE07) with r≈0.8 and b) Peyrusse Vielle (FR13) with r≈0.25.

3.3.2 Mountain stations

As already mentioned in Sect. 2.3.1., mountain stations should be considered with care when used for validation of modelling results. Two stations with the highest altitude in the EMEP domain are used; CH01 and SK02. Annual average at CH01 calculated from observations is $\bar{c}(NO_2)=0.11\,\mu g(N)m^{-3}$, while the corresponding model value is $\bar{c}(NO_2)=0.33\,\mu g(N)m^{-3}$. Further at CH01 extremely low SO_2 values were observed with an average $\bar{c}(SO_2)=0.08\,\mu g(S)m^{-3}$ while the model has $\bar{c}(SO_2)=0.27\,\mu g(S)m^{-3}$ and the following BIAS(SO_2)>200% is found for this station. Low observed $\bar{c}(SO_2)$ on CH01 is expected since it is usually above the ABL height and therefore not affected by the surface SO_2 emission sources. The similar result is found for SK02.

3.3.3 Validation of the Grisogono *K(z)* scheme

In order to find eventual improvements in the EMEP model performance with the change of *K(z)* scheme, differences (*D*) between the old and the new *r* and BIAS values are calculated. Differences are defined as:

$$D(X) = X(\text{Grisogono}) - \text{X(O'Brien)}, \tag{16}$$

and relative differences (*RD*) as:

$$RD(X) = (X(\text{Grisogono}) - \text{X(O'Brien)}) \times 100\%/\text{X(O'Brien)}, \tag{17}$$

where parameter *X* can be *r* or the absolute value of BIAS, ABS (BIAS). For $X=r$, $D(r)>0$ and $RD(r)>0$ means that model performs better with the Grisogono *K(z)* scheme, while for X=BIAS, D(BIAS)>0 and RD(BIAS)>0 denotes that the O'Brien scheme agrees better with the observations. Similarly $D\approx0$ and $RD\approx0$ denotes equally good performance of both schemes.

In order to quantify changes with the new *K(z)* scheme, $RD(r)$ in percentage is given for NO_2 in Fig. 6a. The modelled absolute values and BIAS is very sensitive to the balance between the different processes in the model. Therefore, a smaller BIAS between model and measurements does not necessarily mean that the new scheme is better than the old; it only means that average concentrations determined with the new scheme is closer to the average of the observed concentrations. However, the BIAS can give insight into the general effect of the new scheme on the modelled values. For instance, if the Grisogono parameterization is less diffusive in stable conditions (Jeričević and Večenaj, 2009a) this should lead to higher average concentrations in these cases. The temporal correlation coefficient, however, is a better measure for whether the new scheme provides a better physical description. Therefore, we focus on the changes in the correlation coefficient between model results and observations. Improvements in $r(NO_2)$ up to 30% with the Grisogono scheme are found on 51% stations (mainly at stations in Central Europe) while on 14% stations there was no change in r with the change of *K(z)* scheme, and on 35% stations $r(NO_2)$ is lower with the new scheme (Fig. 6a). Higher increase in $r(SO_2)$ up to 20–50% with the new *K(z)* scheme is found on 54% stations (Fig. 6b), $r(SO_2)$ remained same on 22% stations, while on 24% stations smaller decrease was found. For SO_2 (Fig. 6b) improvement is found on more stations than for NO_2, except stations in Scotland and in the shipping area. There is a generally an increase in $r(SO_4^{-2})$ with the higher improvement around 45% and 20% on Slovakian stations SK02 and SK04 respectively (Fig. 6c). However, stations in the shipping and mountain area mainly did not exhibit improvements in r, except $r(SO_4^{-2})$ increased in mountain area with implementation of the new *K(z)* scheme.

Here, *RD*(BIAS) for NO_2, Fig. 7a, show that on 60% of analyzed stations BIAS(NO_2) is lowered ≈10% with the new *K(z)* scheme. Stations with *RD*(BIAS)>0, i.e. increased BIAS(NO_2) with the Grisogono scheme, are mainly those with an improvement in correlation coefficient except at SE02, SE08, CH01 and DE08. Values of *RD*(BIAS) for SO_2 is represented in Fig. 7b, and mainly improvement is found with the new *K(z)* scheme; on 50% stations BIAS(SO_2) is decreased, on 23% stations there is no change in BIAS(SO_2) values and on 26% stations there is an increase in BIAS(SO_2). For SO_4^{-2} (see Fig. 7c) on nearly 64% stations lower BIAS with *D*(BIAS) ≈−10% is found with the new scheme. Evidently SO_4^{-2} had the most harmonized changes, at most of analyzed stations, with the change of *K(z)* scheme. Spatial distribution of $D(r)$ and D(BIAS) for SO_4^{-2} is shown in Fig. 8a and b, respectively. In Fig. 8a yellow dots represents higher correlation coefficients with the new scheme while in Fig. 8b green dots denotes stations where underestimation of measured sulphate daily surface concentrations are lower with the new *K(z)* scheme. Obviously only few stations, with higher uncertainty in measurements, did not follow the common trend of improvement with the new *K(z)* scheme.

In order to investigate seasonal variability of *K(z)*, represented with the two different schemes, the NO_2 is further analyzed. Yearly course of a) r values, b) BIAS values, c) RMSE and d) average monthly concentrations of NO_2 calculated between the measurements and modelled $c(NO_2)$ values with two *K(z)* schemes, the Grisogono (blue line) and the O'Brien (red line) are represented in Fig. 9. All analyzed stations with $c(NO_2)$ measurements during year 2001 are taken into account. In Fig. 9a systematically higher r values with the new *K(z)* scheme are shown in both: stable conditions more characteristic during the colder part of the year, and unstable conditions during the warmer part of the year. According to BIAS (Fig. 9b), in the warmer part of the year model underestimates $c(NO_2)$ with the both *K(z)* schemes. Furthermore, RMSE in Fig. 9c is also the lowest during the summer time. The measured and modelled mean monthly NO_2 values in Fig. 9d show decrease of $c(NO_2)$ during the warmer part of the year. This drop in $c(NO_2)$ is caused by increased photolysis of NO_2 and more vigorous vertical mixing during the warmer period. Note the higher $c(NO_2)$ values with the new *K(z)* scheme during the warmer part of the year, which shows that the new *K(z)* scheme was less diffusive in more convective conditions than the operational scheme. In Fig. 9d note that average monthly values with both schemes was similar during the colder part of the year, while the second peak in November was not captured with the model. Nevertheless r is higher with the new scheme in winter stable conditions also.

Finally, r and BIAS are also calculated for all stations for the year 2001 between the measured and the modelled $c(NO_2)$, $c(SO_2)$ and $c(SO_4^{-2})$ values. In Fig. 10 yearly scatter plots between measured and modelled daily surface concentrations are shown. For NO_2, r=0.65 with the Grisogono, while r=0.63 is achieved with the O'Brien method. BIAS is similar for NO_2, with the Grisogono method, BIAS=−18% and BIAS=−17% with the O'Brien method. The correlation coefficient r=0.57 is found for SO_2 with the Grisogono while for the O'Brien method r=0.55. According to the BIAS values the model generally overestimates SO_2 around 27% with the Grisogono and 30% with the O'Brien method. It should be pointed out that the stations with large overestimations i.e. mountain and stations under strong influence of shipping, are excluded from this analysis because they are not representative for the model grid-cell. For SO_4^{-2}, result is similar for both methods; $r\approx$0.61 and BIAS$\approx$−12%.

3.4 Verification of the boundary layer height representation in the EMEP model

In the EMEP model schemes for calculation of H, the operational and the new ABL scheme based on Ri_B number are compared. Evaluation was performed on two data sets: (i) radiosoundings from 24 different measuring stations in Europe (Table 1) during January and July in year 2001 and (ii) on vertical temperature and wind measurements in year 2001 from the Cabauw tower.

3.4.1 Radiosouniding data

For January and July in year 2001, r and BIAS values are calculated at available UTC times (Table 1) between H determined from the soundings (H_{sond}), and H calculated from the EMEP model (H_{EMEP}) with the operational scheme (H_{old}), and the Ri_B scheme (H_{new}). Values of H_{sond} are determined with the Ri_B scheme. Figure 11a shows correlation coefficients in January, and for most of the analyzed stations $r\approx$0.5. Lower values of $r\approx$0.3 are found at Torshavn, Legionowo, Practica di Mare and Izmir station (Table 1), and higher values $r\approx$0.7 are found at: Stavanger, Herstmonceux, Uccle and Trappes. While H_{new} shows a slight improvement in r, there is a considerable improvement in BIAS values, see Fig. 11b. The model underestimates H_{sond} with the old scheme (BIAS≈−50%), while with the new ABL scheme the underestimation is significantly lower (BIAS≈−20 %). Overestimations are found for Payerne and Meiningen, for two stations in the Alps area. Figure 11c shows average monthly H which is calculated from soundings ($\bar{H}_{\mathrm{sond}}$), with values 200 m<$\bar{H}_{\mathrm{sond}}$<600 m. The highest $\bar{H}_{\mathrm{sond}}$ are found for the stations located in the Southern Europe e.g. Madrid, La Coruna and Izmir. The only exception among northern stations is Torshavn with a somewhat higher $\bar{H}_{\mathrm{sond}}$. On the other hand, the lowest $\bar{H}_{\mathrm{sond}}$ in January are found for the stations in the Central Europe e.g. Prague, Vienna, Wroclaw and Milan, which is expected, because of long stable conditions during the winter, which occur over the continent and the corresponding $H$are usually low. Average H calculated from the model with the old ($\bar{H}_{\mathrm{old}}$), and the new ($\bar{H}_{\mathrm{new}}$), scheme generally underestimates $\bar{H}_{\mathrm{sond}}$ (see Fig. 11c). Average monthly H values for different stations are in range: 200 m<$\bar{H}_{\mathrm{old}}$ 400 m, while for the new method: 400 m<$\bar{H}_{\mathrm{new}}$<600 m.

Figure 12 shows time series of H in January for four selected locations; two with the higher r Herstmonceux and Stavanger, Fig. 12a and b respectively, and two with the lower r Torshavn and Legionowo, Fig. 12d and c, respectively. For Herstmonceux and Stavanger the agreement between H_{sond} and H_{EMEP} is good, especially with the new ABL scheme. Note a period of low H_{EMEP}≈50 m (Fig. 12b, c and d), simulated in the model which occurred from 13 to 20 January 2001. Simulated lower values of H_{EMEP} are connected with the high pressure system movement across the Northern Europe (not shown), starting from the Island at 13 January 2001 and moving across the Europe to its end position over Russia at 20 January 2001.

For that period at the stations Herstmonceux and Stavanger, H_{sond}≈H_{EMEP}, and Torshaven and Legionowo are $H_{\mathrm{sond}} - H_{\mathrm{EMEP}}$≈1000 m and $H_{\mathrm{sond}} - H_{\mathrm{EMEP}}$≈500 m, respectively. This disagreement between H_{sond} and H_{EMEP} at Torshaven and Legionowo during the stable conditions is the main cause for the corresponding lower r values.

July 2001 over the continent was characterized with convective, unstable conditions during the day time, and strong near surface inversions during the night. Generally, in July r is much higher for the both ABL methods, r≈0.7 (Fig. 13a) as compared with $r \approx 0.5$ (Fig. 11a) in January. During the summer time both ABL methods perform equally well, however slightly better results according to r are found with the old ABL scheme than with the operational ABL scheme employed in the EMEP model. According to BIAS, Fig. 13b, the model underestimates H_{sond} with the similar magnitude with both ABL methods. Note spatial variation of BIAS in July. The lowest BIAS values are found in the Central European area where BIAS≈−20%, see Fig. 13b and the corresponding $\bar{H}_{sond} \approx 800$ m; $\bar{H}_{EMEP}=700$ m, see Fig. 13c. In the Northern Europe BIAS≈−40% and the corresponding $\bar{H}_{sond}=1000$ m; $\bar{H}_{EMEP}=600$ m. The underestimation is the highest in the Southern Europe with BIAS ranging from −60% to −80% where $\bar{H}_{sond}$ obtain the highest values, $\bar{H}_{sond} \approx 1200$ m.

Time series in July (Fig. 14) show diurnal variation of H from the night-time low H in the statically stable conditions toward high daily H values in the convective unstable conditions. The model captures H_{sond} daily variations and good agreement between H_{sond} and H_{EMEP} is found e.g. for Meiningen $r=0.91$ and Madrid $r=0.84$ with the new ABL scheme. Note that, at Lisbon and Torshavn, H_{sond} are significantly higher than H_{EMEP}. The modelled H_{EMEP} were almost constant in time and consequently corresponding lower r and higher BIAS values were found at those stations. Note that BIAS at Lisbon is the highest among all analyzed stations. Lisbon station is located near the boundary of the model domain where the modelled results are dominated by weakly varying boundary conditions. Furthermore, the model was not able to reproduce variability shown in H_{sond} both in January and July at Torshavn station located on the Faroe Islands in the Atlantic Ocean. The Faroe Islands are situated entirely within one grid cell in the model and the model was incapable to realistically represent H in the complex coastal orography due to still relatively low model resolution.

3.4.2 The ABL height calculated from the Cabauw data

In this section procedure of deriving H with the Ri_B number method from the Cabauw measurements is firstly described. Following, average hourly vertical profiles of Ri_B

number, $(\overline{Ri_B(z_j,t)})$, where j=10, 20,..., 200 m are the measuring levels; and the corresponding H are analyzed and described for every month in year 2001 (Fig. 15).

As mentioned boundary layer height from the Cabauw data (H_{tower}) is determined with theRi_B method. Vertical profiles of the Ri_B number are calculated from the temperature and the wind measured at every tower level with the time interval Δt=10 min during year 2001. In this way the sequence of $Ri_B(z,t)$ values for the year 2001 is produced and monthly averaged to obtain Ri_B daily courses, $(\overline{Ri_B(z_j,t)})$ for every month in year 2001 (Fig. 15). It is relatively easy to follow daily and seasonal variations of H by looking at the Ri_{BC}=0.25 (the top of blue area in Fig. 15).

The analysis of $\overline{Ri_B(z_j,t)}$ provide good insight in processes of development and decay of the CBL and the SBL in different times of the year. The occurrence of the morning and the afternoon transition layer, characterized with a sudden and rapid decay/increase of the CBL, is also shown. In January, Fig. 15a, during the night-time H is often less than 100 m. Daily development of H starts after 10:00 a.m. reaching the maximum $H\approx$200 m at 01:00 p.m. and lasting approximately 1 h after which H decreased. In February, Fig. 15b night-time H is higher than in January, ranging between 100 and 200 m, the CBL starts to develop around 08:00 a.m. reaching the maximum in the period between noon and 02:00 p.m. In February the afternoon transition layer occurred around 03:00 p.m.. Note that the transition layer has similar characteristics for the most of the analyzed months in year 2001. In following spring and summer months from March, Fig. 15c, to August, Fig. 15h, the CBL is progressively intensifying, becoming more and more unstable. In the warmer part of the year the CBL lasted longer, which is expected since the CBL is correlated with the incoming solar radiation. Note appearance of the areas with $\overline{Ri_B(z_j,t)}$<0 numbers (yellow area in Fig. 15) in April and becoming largest in June, Fig. 15f. During the SBL conditions, in the warmer part of the year, strong near surface inversions and weak winds are measured in the surface layer. In the nigh-time SBL conditions, $Ri_B(z_j,t)\gg Ri_{BC}$ (white areas in Fig. 15) is found and corresponding H is extremely shallow. In September and October periods stable conditions prevails and SBL is 100 m–150 m thick. In November and December, Fig. 15l and Fig. 15m, respectively, dominantly stable conditions with mostly $\overline{Ri_B(z,t)}>0$ numbers are present. Unstable conditions occur from 10:00 a.m. to 14:00 p.m. and the average H is only 50 m.

In Fig. 16 monthly correlation coefficients calculated between the H determined from the measurements,H_{tower}, and the modelled values determined with the operational and Ri_B number method; H_{old} (red) and H_{new} (blue), respectively. Obviously the new ABL scheme gives significantly better results for all months except for June, July and August i.e. the summer period when both schemes performed equally well in the surface layer. Since at the Cabauw tower there are no measurements above 200 m, during the strong CBL conditions it was only possible to investigate correlations regarding time evolution of the ABL and the strength of turbulence in the lowest part of the ABL. Higher vertical measurements would provide more information and help distinguish between performances of the two ABL schemes. Nevertheless, higher correlation coefficients and similar performance of the two schemes during the warmer part of the year is in agreement with the radiosoundings results, which showed that the ABL scheme based on Ri_B number method performs better in stable conditions than the operational one.

4 Conclusions

The new *K(z)* and the ABL schemes were implemented in the EMEP model. Prior to incorporation in the model vertical profiles of *K(z)* have been analyzed on the LES data (DATABASE64; Esau and Zilitinkevich, 2006) and better performance of the Grisogono scheme is established in stable atmospheric conditions. Further, evaluation of the model performance based on r and BIAS on all EMEP stations in year 2001 was conducted for the operational and the new model setup. Uncertainties in the observations are taken into account in order to find the models ability to reproduce spatial variability in simulation of different chemical species. However, it should be pointed that the model BIAS is an overall measure for improvement evaluation since it is very sensitive too changes in parameterization and the modelled absolute values can easily be right for the wrong reasons. Therefore, with respect to model performance for NO_2, SO_2 and SO_4^{-2} the conclusions are based on the changes in correlation coefficients between observations and model results. Main conclusions are:

- The EMEP model shows moderate improvement in r for NO_2 and SO_2 and slight improvement for SO_4^{-2} for most of the analyzed stations. The $r(NO_2)$ is improved nearly 30% on 51% of analyzed stations, while $r(SO_2)$ with the Grisogono scheme have an increase from 10% up to 50% on 54% of stations. For sulphate there is an increase in $r(SO_4^{-2})$ from 5 to 10%. Yearly scatter plots between measured and modelled daily surface concentrations at all analyzed stations except those with higher uncertainties in measurements show improvement in correlation coefficient from 0.63 to 0.65 for NO_2, and from 0.55 to 0.57 for SO_2 with the new scheme. For SO_4^{-2} correlation coefficient is around 0.61 with both schemes.

- Based on the LES data it is found that the Grisogono scheme is generally less diffusive, which is an important preference especially in stable atmospheric conditions. Underestimation of sulphate is also generally lower on most of the analyzed stations with the new scheme. The proposed Grisogono scheme is recommended for application due to its scientific and technical advantages (when remaining within the first-order closure schemes) since it demands only two input variables instead of four as in the O'Brien scheme. In practical implementations e.g. in air quality modelling, both schemes depend on capabilities of used meteorological drivers as well as on model's horizontal and vertical grid resolution. Therefore improvements in the NWP model performance would yield to appreciable difference in terms of both, magnitude and spatial distribution of pollutants.

- Stations which are more affected by the local emission sources, as well as mountain stations do not show significant improvement with the change of the *K(z)* scheme. On those stations the magnitude of the error was much higher than the magnitude of the variability resulting from the change of the *K(z)* scheme. These results indicate that higher horizontal resolution, as well as better defined emissions is needed in order to be able to simulate air pollution transport in a complex coastal terrain under the influences of local sources.

– The ABL height, H, calculated with the EMEP model is in a good agreement with the radiosounding measurements from different stations in Europe. The EMEP model is able to reproduce spatial and temporal variability of H, with r from 0.7 to 0.9 during convective conditions, and r from 0.4 to 0.6 in stable conditions with the both ABL schemes. However, the new ABL scheme based on the Ri_B number performs better in the stable conditions compared to the method based on the Blackadar *K(z)* profiles which is also confirmed with significantly lower BIAS values.

– Results of the intercomparison between the modelled and the ABL heights derived from the Cabauw data reveal systematic improvement with the new ABL scheme especially during the colder part of the year (Fig. 16).

This comprehensive evaluation study of different *K(z)* and ABL schemes applied in the EMEP model provides a basis for further model evaluation and development within the frame of the EMEP4HR project.

Acknowledgements. The authors are grateful to Leonor Tarrasón on support, discussions and ideas in performance of this work. Željko Večenaj gave important contribution in analyzing the LES data, and Fred Bosveld from the Royal Netherlands Meteorological Institute is appreciated for providing the measurements from the Cabauw tower. The EMEP4HR project is under number 175183/S30 funded by the Research Council of Norway. The work is partly supported by the Croatian Ministry of Science, Education and Sport under project numbers BORA 119-1193086-1311, 004-1193086-3036 and 119-1193086-1323. The work of H. Fagerli was supported by the European Monitoring and Evaluation Programme (EMEP) under UNECE, and partially by EU NitroEurope IP (contract 017841).

References

Athanassiadis, G., Trivikrama, R., Jia-Yeong, K., and Clarc, R.: Boundary layer evolution and its influence on ground level ozone concentrations, Environ. Fluid Mech., 2(4), 339–357, doi:10.1023/A:102456018087, 2002.

Bartnicki, J., Gusev, A., Barrett, K., and Simpson, D.: Atmospheric Supply of Nitrogen, Lead, Cadmium, Mercury and Dioxins/Furans to the Baltic Sea in 1996–2000, Joint MSC-W & NILU Note 6/02, for the Helsinki Commission (HELCOM), Baltic Marine Environment Protection Commission, 2002.

Beljaars, A. C. M. and Bosveld, F. C.: Cabauw data for the validation of land surface parameterization schemes, J. Climate, 10(6), 1172–1193, doi:10.1175/1520-0442(1997)010<1172;CDFTVO>2.0.CO;2, 1997.

Berge, E. and Jakobsen, H. A.: A regional scale multi-layer model for the calculation of long-term transport and deposition of air pollution in Europe, Tellus, 50, 205–223, doi:10.1034/j.1600-0889.1998.t01-2-00001.x, 1998.

Biswas, J. and Rao, T.: Uncertainties in episodic ozone modeling stemming from uncertainties in the meteorological fields, J. Appl. Meteorol., 40, 117–136, doi:10.1175/1520-0450(2001)040<0117:UIEOMS>2.0.CO;2, 2000.

Blackadar, A. K.: Modeling pollutant transfer during daytime convection. In: Fourth Symposium on Atmospheric Turbulence Diffusion and Air Quality, AMS, Reno, NV, USA, 443–447, 1979.

Chen, T. H., Henderson-Sellers, A., Milly, P. C. D., Pitman, A., Beljaars, A. C. M., Abramopoulos, F., Boone, A., Chang, S., Chen, F., Dai, Y., Desborough, C., Dickinson, R., Duemenil, L., Ek, M., Garratt, J., Gedney, N., Gusev, Y., Kim, J., Koster, R., Kowalczyk, E., Laval, K., Lean, J., Lettenmaier, D., Liang, X., Mengelkamp, T.-H., Mahfouf, J.-F., Mitchell, K., Nasonova, O., Noilhan, J., Polcher, J., Robock, A., Rosenzweig, C., Schaake, J., Schlosser, C. A., Schulz, J. P., Shao, Y., Shmakin, A., Verseghy, D., Wetzel, P., Wood, E., Xue, Y., Yang, Z.-L., and Zeng, Q.-C.: Cabauw experimental results from the Project for Intercomparison of Land-surface Parameterization Schemes (PILPS), J. Climate, 10, 1194–1215, doi:10.1175/1520-0442(1997)010<1194;CERFTP>2.0.CO;2, 1997.

Deardorff, J. W.: Parameterization of the planetary boundary layer for use in general circulation model, Mon. Weather Rev., 100, 93–106, doi:10.1175/1520-0469(19729029<0091:NIONAU>2.0.CO;2, 1972.

Ek, M. B. and Holtslag, A. A. M.: Evaluation of a land-surface scheme at Cabauw, Theor. Appl.

Climatol., 80, 213–227, doi:10.1007/S00704-004-0101-4, 2005.
ENVIRON: User's Guide to the Comprehensive Air Quality Model with Extensions (CAMx) Version 2.00. ENVIRON International Corporation, 101 Rowland Way, Suite 220, Novato, California, USA, 94945-5010, online available at: http://www.camx.com/, 1998.
Esau, I. and Zilitinkevich, S. S.: Universal dependences between turbulent and mean flow parameters in stably and neutrally stratified planetary boundary layers, Nonlinear Proc. Geoph., 13, 122–144, 2006.
Fagerli, H. and Eliassen, A.: Modified parametrization of vertical diffusion, in: Transboundary Acidification, Eutrophication and Ground Level ozone in Europe, EMEP Summary Status Report 2002, Joint CCC & MSC-W Research Report No. 1&2/01, Norwegian Meteorological Institute, Oslo, Norway, 74 pp., online available at: http://emep.int/publ/common_publications.html#2003, 2002.
Fagerli, H., Simpson, D., and Aas, W.: Model performance for sulphur and nitrogen compounds for the period 1980 to 2000, In L. Tarrasón, Editor, Transboundary Acidification, Eutrophication and Ground Level Ozone in Europe. EMEP Status Report 1/2003, Part II Unified EMEP Model Performance, The Norwegian Meteorological Institute, Oslo, Norway, 66 pp., 2003.
Fagerli, H., Simpson, D., and Tsyro, S.: Unified EMEP model: Updates. In EMEP Report 1/2004, Transboundary acidification, eutrophication and ground level ozone in Europe, Status Report 1/2004, The Norwegian Meteorological Institute, Oslo, Norway, 11–18, 2004.
Fagerli, H., Legrand, M., Preunkert, S., Simpson, D., Vestreng, V., and Cerqueira, M.: Modeling historical long-term trends of sulfate, ammonium and elemental carbon over Europe: A comparison with ice core records in the Alps, J. Geophys. Res., 112, D23S13, doi:10.1029/2006JD008044, 2007.
Fagerli, H. and Aas, W.: Trends of nitrogen in air and precipitation: Model results and observations at EMEP sites in Europe, 1980–2003, Environ. Pollut., 154, 448–461, doi:10.1016/j.envpol.2008.01.024, 2008.
Fay, B., Schrodin, R., Jacobsen, I., and Engelbart, D.: Validation of mixing heights derived from the operational NWP models at the German Weather Service, in: The determination of the mixing height – current progress and problems, EURASAP Workshop Proceedings 1–3 October 1997, edited by: Gryning, S.-E., Report Risø-R-997 (EN), ISBN 87-550-2325-8, Risø National Laboratory, Roskilde, Denmark, 55–58, 1997.
Garratt, J. R: The atmospheric boundary layer, Cambridge University Press, UK, 316, 1992.
Grisogono, B.: A generalized Ekman layer profile within gradually-varying eddy diffusivities, Q.

J. Roy. Meteorol. Soc., 121, 445–453, 1995.

Grisogono, B. and Oerlemans, J.: A theory for the estimation of surface fluxes in simple katabatic flows, Q. J. Roy. Meteorol. Soc., 127, 2725–2739, 2001.

Grisogono, B. and Oerlemans, J.: Justifying the WKB approximation in pure katabatic flows, Tellus A, 54, 453–462, doi:10.1034/j.1600-0870.2002.201399.x, 2002.

Grisogono, B., Kraljević, L., and Jeričević, A.: The low-level katabatic jet height versus Monin-Obukhov height, Q. J. Roy. Meteorol. Soc., 133, 2133–2136, 2007.

Grisogono, B. and Belušić, D.: Improving mixing length-scale for stable boundary layers, Q. J. Roy. Meteorol. Soc., 134, 2185–2192, 2008.

Gryning, S.-E. and Batchvarova, E.: Marine boundary layer and turbulent fluxes over the Baltic sea: measurements and modelling, Bound.-Lay. Meteorol., 103, 29–47, 2002.

Holtslag, A. A. M. and Moeng, C. H.: Eddy diffusivity and countergradient transport in the convective atmospheric boundary layer, J. Atmos. Sci., 48, 1690–1698, doi:10.1175/1520-0469(1991)048<1690:EDACTI>2.0.CO;2, 1991.

Holtslag, A. A. M. and Boville, B. A.: Local versus nonlocal boundary-layer diffusion in a global climate model, J. Climate, 6, 1825–1842, doi:10.1175/1520-0442(1993)006<1825:LVNBLD>2.0.CO;2, 1993.

Ivatek-Šahdan, S. and Tudor, M.: Use of high-resolution dynamical adaptation in operational suite and research impact studies, Meteorol. Z., 13(2), 99–108, 2004.

Jakobsen, H. A., Berge, E., Iversen, T., and Skalin, R.: Status of the development of the multilayer Eulerian model, EMEP/MSC-W Note 3/95, online available at: http://www.emep.int/mscw/mscw_publications.html#1995, 1995.

Jeričević, A. and Grisogono, B.: The critical bulk richardson number in urban areas: verification and application in a numerical weather prediction model, Tellus A, 58, 19–27, doi:10.1111/j.1600-0870.2006.00153.x, 2006.

Jeričević, A., Kraljević, L., Vidič, S., and Tarrasón, L.: Project description: High resolution environmental modelling and evaluation programme for Croatia (EMEP4HR), Geofizika, 24(2), 137–143, online available at: http://geofizika-journal.gfz.hr/vol24.htm, 2007.

Jeričević A. and Večenaj, Ž.: Improvement of vertical diffusion analytic schemes under stable atmospheric conditions, Bound.-Lay. Meteorol., 131, 293–307, doi:10.1007/s10546-009-9367-5, 2009.

Jonson, J. E., Bartnicki, J., Olendrzynski, K., Jakobsen, H. A., and Berge, E.: EMEP Eulerian model for atmospheric transport and deposition of nitrogen species over Europe, Environ.

Pollut., 102, 289–298, 1998.
Jonson, J. E., Simpson, D., Fagerli, H., and Solberg, S.: Can we explain the trends in European ozone levels?, Atmos. Chem. Phys., 6, 51–66, 2006, http://www.atmos-chem-phys.net/6/51/2006/.
Klaić, Z.: A lagrangian one-layer model of long-range transport of SO_2, Atmos. Environ., 24A, 1861–1867, 1990.
Klaić, Z.: A lagrangian model of long-range transport of sulphur with the diurnal variations of some model parameters, J. Appl. Meteorol., 35, 574–586, 1995.
Klaić, Z. and Beširević, S.: Modelled sulphur depositions over Croatia, Meteorol. Atmos. Phys., 65, 133–138, 1998.
Kraljević, L., Belušić, D., Bencetić Klaić, Z., Bennedictow, A., Fagerli, H., Grisogono, B., Jeričević, A., Mihajlović, D., Špoler Čanić, K., Tarrasón, L., Valiyaveetil, S., Vešligaj, D., and Vidič, S.: Application of EMEP Unified model on regional scale – EMEP4HR, Proceedings from a 12 HARMO conference Part 1: Oral Presentations, Đuričić, V. (ed.), Zagreb, Croat. Meteorol. J., 43, 151–151, online available at: http://www.harmo.org/Conferences/Proceedings/_Cavtat/topicIndex.asp?topicID=0, 2008.
Lee, H. N. and Larsen, R. J.: Vertical diffusion in the lower atmosphere using aircraft measurements of 222Rn, J. Appl. Meteorol., 36, 1262–1270, doi:10.1175/1520-0450(1997)036<1262:VDITLA>2.0.CO;2, 1997.
Louis, J. F.: A parametric model of vertical eddy fluxes in the atmosphere, Bound.-Lay. Meteorol., 17, 187–202, 1979.
Mahrt, L.: Modelling the depth of the stable boundary layer, Bound.-Lay. Meteorol., 21, 3–19, 1981.
Mahrt, L.: Stratified Atmospheric Boundary Layers, Bound.-Lay. Meteorol., 90, 375–396, doi:10.1023/A:1001765727956, 1999.
Mahrt, L.: The influence of nonstationarity on the turbulent flux-gradient relationship for stable stratification, Bound.-Lay. Meteorol., 125, 245–264, doi:10.1007/s10546-007-9154-0, 2007.
Matthias, V., Aulinger, A., and Quante, M.: Adapting CMAQ to investigate air pollution in North Sea coastal regions, Environ. Modell. Softw., 23, 356–368, doi:10.1016/j.envsoft.2007.04.010, 2008.
Mauritsen, T., Svensson, G., Zilitinkevich, S., Esau, I., Enger, L., and Grisogono, B.: A total turbulent energy closure model for neutrally and stably stratified atmospheric boundary layers, J. Atmos. Sci., 64, 4113–4126, doi:10.1175/2007JAS2294.1, 2007.

McNider, R. T. and Pielke, R. A.: Diurnal boundary layer development over sloping terrain, J. Atmos. Sci., 38, 198–2212, doi:10.1175/1520-0469(1981)038<2198:DBLDOS>2.0.CO;2, 1981.

Monin, A. S. and Obukhov, A. M.: Basic laws of turbulent mixing in the surface layer of the atmosphere, Tr. Geofiz. inst. Akad. Nauk SSSR, 151, 163–187, 1954.

Nowacki, P., Samson, P. J., and Sillman, S.: Sensitivity of Urban Airshed Model (UAM-IV) Calculated Air Pollutant Concentrations to the Vertical Diffusion Parametrisation During Convective Meteorological Situations, J. Appl. Meteorol., 35, 1790–1803, doi:10.1175/1520-0450(1996)035<1790:SOUAMI>2.0.CO;2, 1996.

O'Brien, J. J.: A Note on the vertical structure of the eddy exchange coefficient in the planetary boundary layer, J. Atmos. Sci., 27, 1213–1215, doi:10.1175/1520-0469(1970)027<1213:ANOTVS>2.0.CO;2, 1970.

Olivié, D. J. L., van Velthoven, P. F. J., and Beljaars, A. C. M.: Evaluation of archived and off-line diagnosed vertical diffusion coefficients from ERA-40 with 222Rn simulations, Atmos. Chem. Phys., 4, 2313–2336, 2004, http://www.atmos-chem-phys.net/4/2313/2004/.

Pahlow, M., Parlange, M. B., and Porté-Agel, F.: On Monin-Obukhov similarity in the stable atmospheric boundary layer, Bound.-Lay. Meteorol., 99, 225–248, doi:10.1023/A:1018909000098, 2001.

Poulos, G. S. and Burns, S. P.: An evaluation of bulk Ri-based surface layer flux formulas for stable and very stable conditions with intermittent turbulence, J. Atmos. Sci., 60, 2523–2537, doi:10.1175/1520-0469(2003)060<2523:AEOBRS>2.0.CO;2, 2003.

Schäfer, K., Emeis, S., Hoffmann, J., and Jahn C.: Influence of mixing height upon air pollution in urban and suburban areas, Meteorol. Z., 15, 647–658, 2006.

Seibert, P., Beyrich, F., Gryning, S.-E., Joffre, S., Rasmussen, A., and Tercier, Ph.: Review and intercomparison of operational methods for the determination of the mixing height, Atmos. Environ., 34, 1001–1027, doi:10.1016/S1352-2310(99)00349-0, 2000.

Seinfield, J. H. and Pandis, S. N.: Atmospheric chemistry and physic: from air polution to climate change, John Wiley and Sons, Inc., New York, USA, 1326 pp., 1998.

Simpson, D., Fagerli, H., Jonson, J. E., Tsyro, S., Wind, P., and Tuovinen, J.-P.: The EMEP Unified Eulerian Model. Model Description. Technical Report EMEP MSC-W Report 1/2003, The Norwegian Meteorological Institute, Oslo, Norway, 2003.

Simpson, D., Butterbach-Bahl, K., Fagerli, H., Kesik, M., and Skiba, U.: Deposition and Emis-

sions of Reactive Nitrogen over European Forests: A Modelling Study, Atmos. Environ., 40(29), 5712–5726, 2006a.
Simpson, D., Fagerli, H., Hellsten, S., Knulst, J. C., and Westling, O.: Comparison of modelled and monitored deposition fluxes of sulphur and nitrogen to ICP-forest sites in Europe, Biogeosciences, 3, 337–355, 2006b, http://www.biogeosciences.net/3/337/2006/.
Simpson, D., Yttri, K. E., Klimont, Z., Kupiainen, K., Caseiro, A., Gelencs'er, A., Pio, C., and Legrand, M.: Modeling carbonaceous aerosol over Europe. Analysis of the CARBOSOL and EMEP EC/OC campaigns, J. Geophys. Res., 112, D23S14, doi:10.1029/2006JD008158, 2007.
Sørensen, J. H., Rasmussen, A., and Svensmark, H.: Forecast of atmospheric boundary-layer height for ETEX real-time dispersion modelling, Phys. Chem. Earth, 21, 435–439, doi:10.1016/SOO79-1946(97)81138-x, 1996.
Stull, R. B.: An Introduction to Boundary Layer Meteorology, Kluwer Academic Publishers, Dordrecht, The Netherlands, 666 pp., 1988.
Tsyro, S., Simpson, D., Tarrasón, L., Klimont, Z., Kupiainen, K., Pio, C., and Yttri, K. E.: Modeling of elemental carbon over Europe, J. Geophys. Res., 112, D23S19, doi:10.1029/2006JD008164.2, 2007.
Troen, I. B. and Mahrt, L.: A simple model of the atmospheric boundary layer; sensitivity to surface evaporation, Bound.-Lay. Meteorol., 37, 129–148, doi:10.1007/BF00122760, 1986.
van Ulden, A. P. and Wieringa, J.: Atmospheric boundary layer research at Cabauw, Bound.-Lay. Meteorol., 78, 39–69, doi:10.1007/BF00122486, 1996.
Vieno, M., Dore, A. J., Wind, P., Di Marco, C., Nemitz, E., Phillips, G., Tarrasón, L., and Sutton, M. A.: Application of the EMEP Unified Model to the UK with a horizontal resolution of $5\times5\,km^2$, in: Atmospheric ammonia: Detecting emission changes and environmental impacts, edited by: Sutton, M. A , Baker, S., and Reis, S., Springer, 367–372, 2009a.
Vieno, M., Dore, A. J., Stevenson, D. S., Doherty, R., Heal, M., Reis, S., Hallsworth, S., Tarrasón, L., Wind, P., Fowler, D. Simpson, D., and Sutton, M. A.: Modelling surface ozone during the 2003 heat wave in the UK, Atmos. Chem. Phys., submitted, 2009b.
Zilitinkevich, S. and Calanca, P.: An extended theory for the stably stratified atmospheric boundary layer, Q. J. Roy. Meteorol. Soc., 126, 1913–1923, doi:10.1256/smsqj.56617, 2000.
Zilitinkevich, S. and Baklanov, A.: Calculation of the height of the stable boundary layer in practical applications, Bound.-Lay. Meteorol., 105, 389–409, doi:10.102376832738, 2002.

Zilitinkevich, S., Elperin, T., Kleorin, N., Rogachevskii, I., Esau, I., Mauritsen, T., and Miles, M.: Turbulence energetics in stably stratified geophysical flows: strong and weak mixing regimes, Q. J. Roy. Meteorol. Soc., 134, 793–799, doi:101002/qj.264, 2008.
Zhang, Y., Pun B., Wu, S.-Y., Vijayaraghavan, K., and Seigneur, C.: Application and evaluation of two air quality models for particulate matter for a southeastern U. S. episode, J. Air Waste Manage., 54, 1478–1493, 2004.
Žagar, M. and Rakovec, J.: Small scale surface wind prediction using dynamical adaptation, Tellus A, 51, 489–504, doi:10.1034/j.1600-0870.1999.t01-4-00003.x, 1999.

ACPD
9, 9597–9645, 2009

Title Page
Abstract | Introduction
Conclusions | References
Tables | Figures
◄ | ►
Back | Close
Full Screen / Esc
Printer-friendly Version
Interactive Discussion

Table 1. List of radio sounding stations over Europe used for validation of the ABL height, H, from the EMEP model in January and July 2001. Station name, coordinates, country and observational terms according to UTC are given.

Station	Coordinates	Country	Altitude(m)	UTC
Gothenburg	57.67 N, 12.32 E	Sweden	164	00 and 12
Orland	63.70 N, 9.6 E	Norway	10	00 and 12
Stavanger	63.70 N, 9.6 E	Norway	37	00 and 12
Oslo	60.2 N, 11.08 E	Norway	201	06
Torshavn	62.20 N, 6.77 E	Denmark	56	00 and 12
Hillsborough	54.8 N, 6.17 W	UK	38	00, 06, 12 and 18
Hearstmonceux	50.9 N, 0.32 E	UK	0	00 and 12
Lisbon	38.77 N, 9.13 W	Portugal	105	00 and 12
Zagreb	45.82 N, 16.03 E	Croatia	128	00 and 12
Payerne	46.82 N, 6.95 E	Switzerland	491	00 and 12
Meiningen	50.57 N, 10.37 E	Germany	453	00 and 12
Vienna	48.25 N, 16.87 E	Austria	200	00 and 12
Trappes	48.77 N, 2.02 E	France	168	00 and 12
Legionowo	52.4 N, 20.97 E	Poland	96	00 and 12
Uccle	50.8 N, 4.35 E	Belgium	104	00 and 12
Izmir	30.43 W, 27.17 E	Turkey	29	00 and 12
La Coruna	43.73 N, 8.42 W	Spain	67	00 and 12
Madrid	40.45 N, 3.55 W	Spain	633	00 and 12
Practica di Mare	41.46 N, 12.43 W	Italy	32	00, 06, 12 and 18
Wroclaw	51.13 N, 16.98 E	Poland	122	00 and 12
Copenhagen	55.77 N, 12.53 E	Denmark	42	00 and 12
Prague	50 N, 14.45 E	Czech Republic	303	00, 06, 12 and 18
Milan	45.43 N, 9.28 E	Italy	103	00, 06, 12 and 18

ACPD
9, 9597–9645, 2009

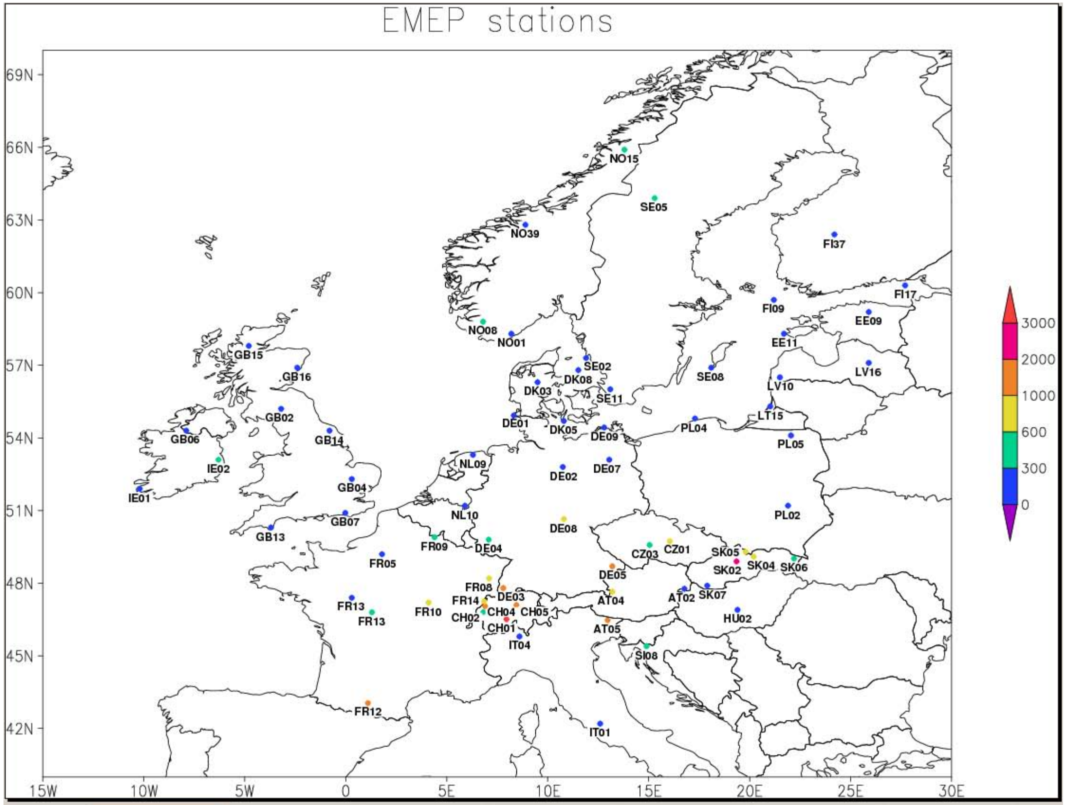

Fig. 1. Stations used for evaluation of the EMEP model performance. Station altitude is represented with different colours ranging from less than 300 m (blue) to higher than 3000 m (red).

ACPD
9, 9597–9645, 2009

Title Page
Abstract
Introduction
Conclusions
References
Tables
Figures
◀◀
▶▶
◀
▶
Back
Close
Full Screen / Esc
Printer-friendly Version
Interactive Discussion

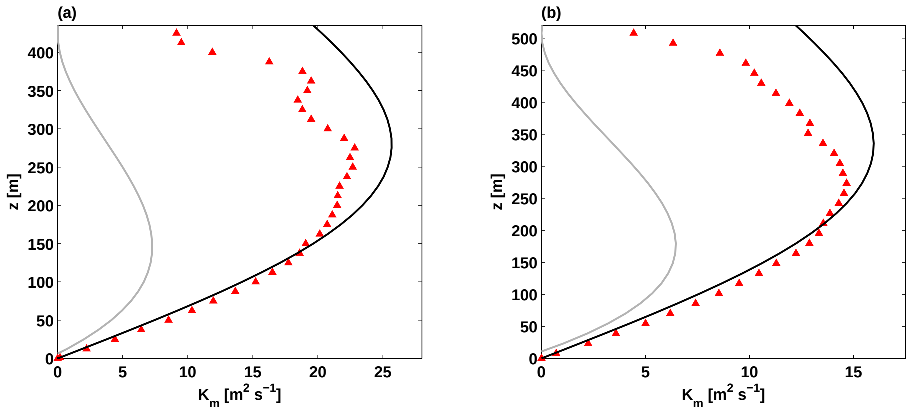

Fig. 2. Vertical profiles of mechanical eddy diffusivity K_m calculated with the O'Brien (grey solid line) and Grisogono method (black solid line) against K_m from the LES data (red triangles) for: **(a)** the nocturnal conditions and **(b)** long-lived stable conditions.

ACPD
9, 9597–9645, 2009

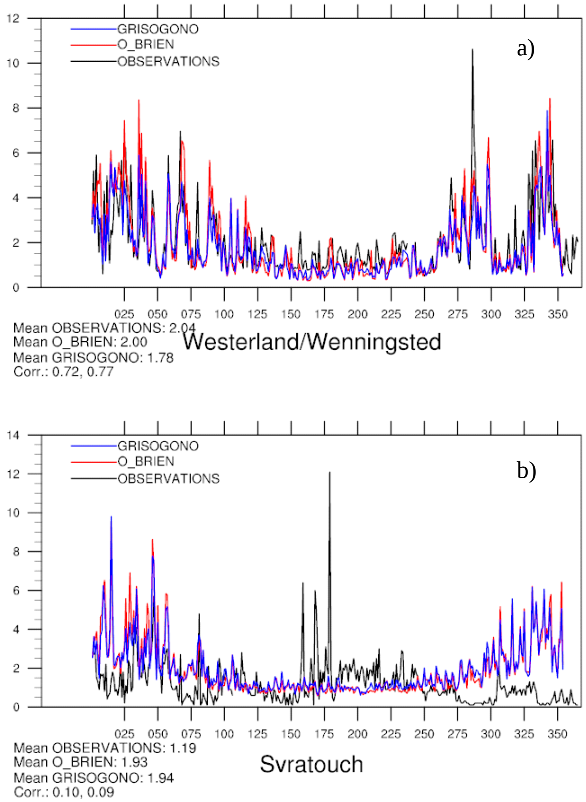

Fig. 3. Time series of the measured (black line) and the modelled daily surface NO_2 concentrations (μg(N)m^{-3}) for: **(a)** Westerland (DE01) and **(b)** Svratouch (CZ01) in year 2001. Modelled results are obtained with two different vertical diffusion schemes: O'Brien (red line) and Grisogono (blue line). Time is given on x-axes in Julian days.

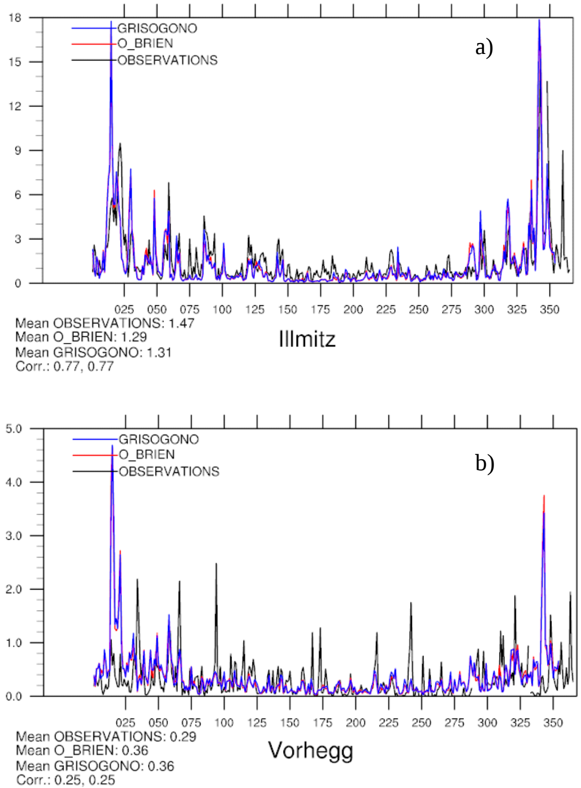

Fig. 4. Same as Fig. 3 but for SO_2 ($\mu g(S) m^{-3}$) on the stations: **(a)** Ilmitz (AT02) and **(b)** Vorhegg (AT05).

ACPD

9, 9597–9645, 2009

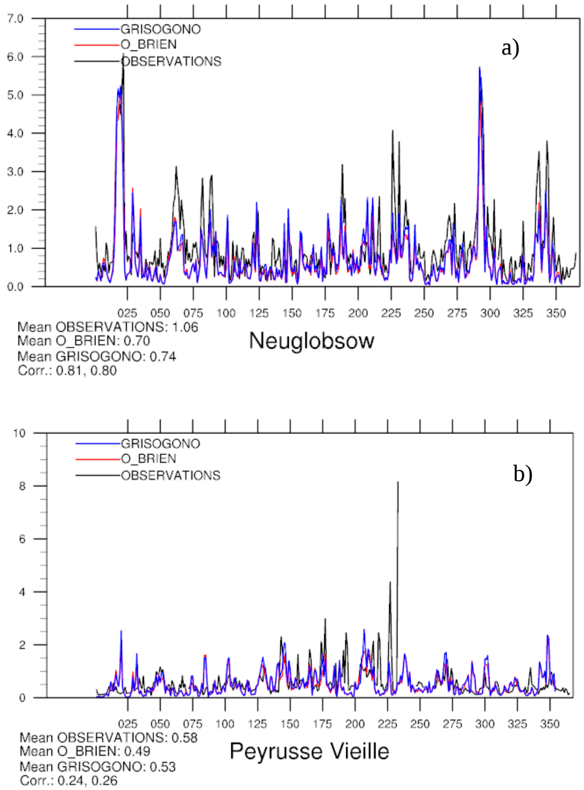

Fig. 5. Same as Fig. 3 but for SO_4^{-2} (μg(S)m^{-3}) on the stations: **(a)** Neuglobsow (DE07) and **(b)** Peyrusse Vielle (FR13).

ACPD

9, 9597–9645, 2009

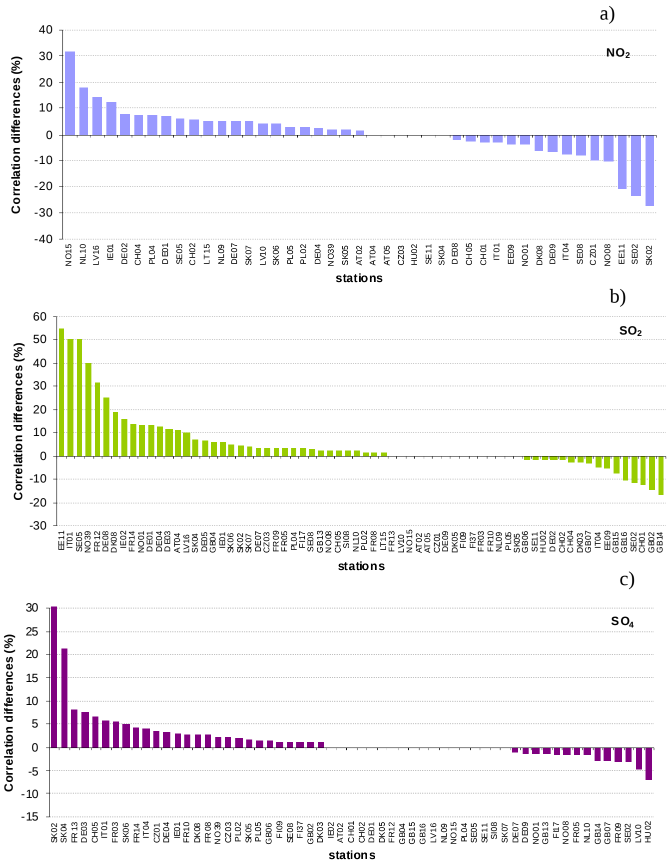

Fig. 6. Relative differences in correlation coefficients, $RD(r)$, calculated between the two EMEP modelled data sets and the observations from the EMEP stations in year 2001 for: **(a)** NO_2, **(b)** SO_2 and **(c)** SO_4^{-2}. Values $RD(r)>0$ denotes better performance of the Grisogono scheme.

ACPD

9, 9597–9645, 2009

Parameterization of vertical diffusion

A. Jeričević et al.

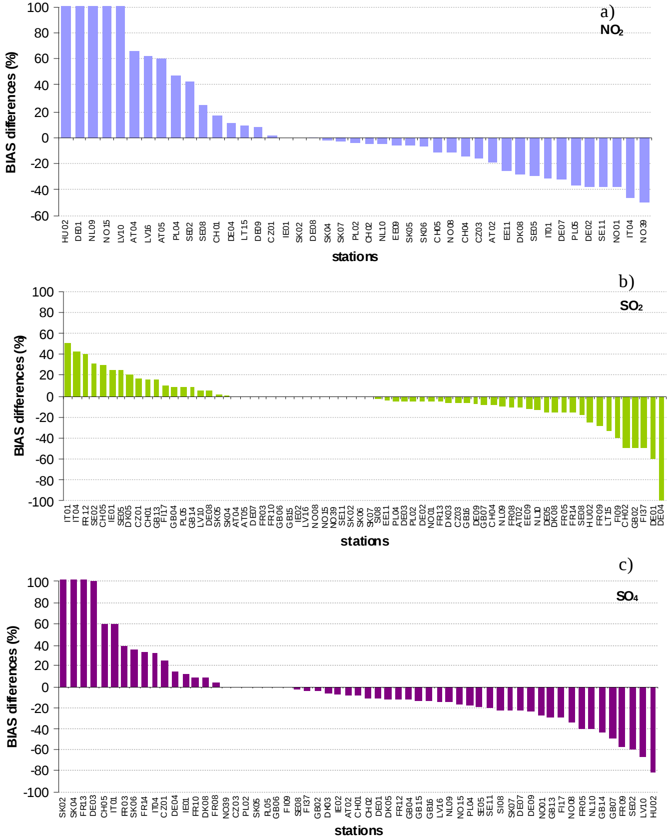

Fig. 7. Same as in Fig. 6 but for relative differences in BIAS, *RD*(BIAS). Values *RD*(BIAS)<0 denotes better performance of the Grisogono scheme.

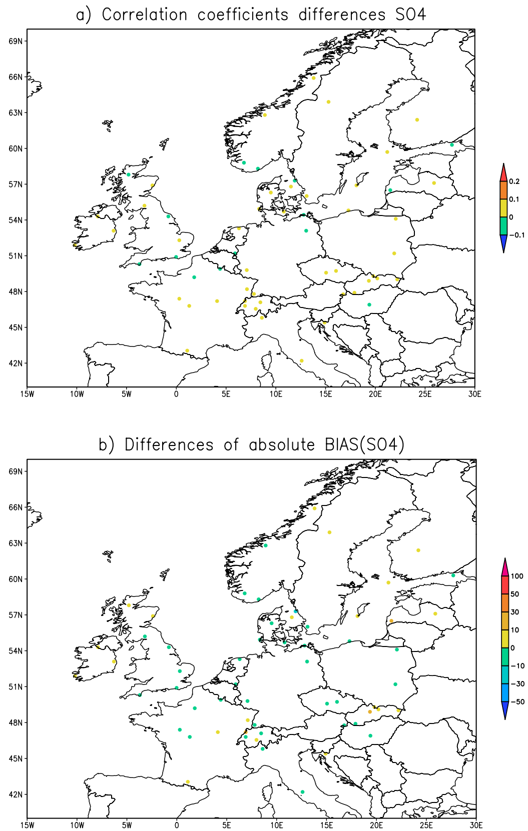

Fig. 8. Differences in **(a)** correlation coefficient, $D(r)$, and **(b)** BIAS values, $D(\text{BIAS})$ calculated between the modelled and measured daily surface SO_4^{-2} concentrations determined with the two different vertical diffusion schemes, the O'Brien and Grisogono, for year 2001. Values $D(r)>0$ and $D(\text{BIAS})<0$ denotes better performance of the Grisogono scheme.

ACPD
9, 9597–9645, 2009

Title Page
Abstract
Introduction
Conclusions
References
Tables
Figures
◀I
▶I
◀
▶
Back
Close
Full Screen / Esc

Printer-friendly Version

Interactive Discussion

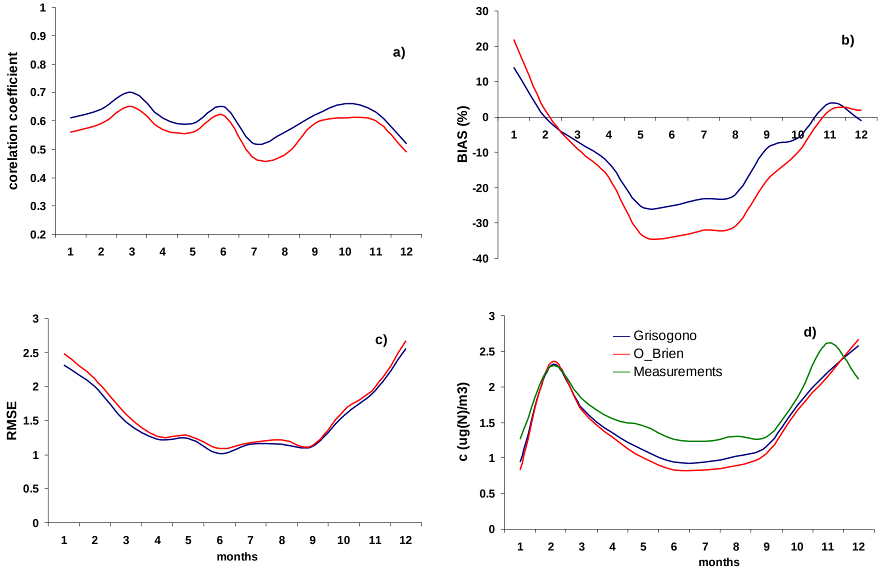

Fig. 9. Annual course of: **(a)** r, **(b)** BIAS, **(c)** RMSE between the measured and modelled $c(NO_2)$ and **(d)** average monthly $c(NO_2)$ values in year 2001. Two different *K(z)* schemes were used O'Brien (red) and Grisogono (blue), monthly averages calculated from observations are marked with green line **(d)**.

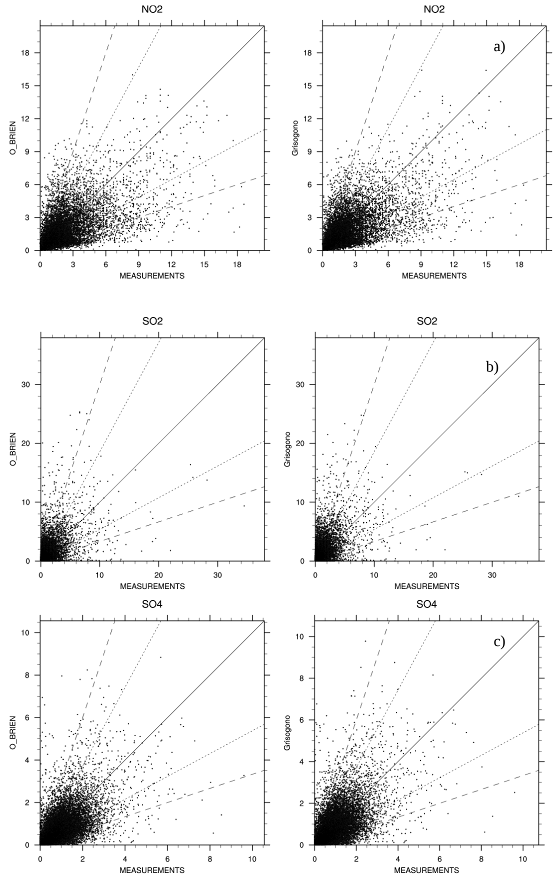

Fig. 10. Annual scatter plots between the measured and modelled **(a)** $c(NO_2)$, **(b)** $c(SO_2)$ and **(c)** $c(SO_4)$ values. Modelled concentrations are determined with two *K(z)* schemes: O'Brien (left panel) and Grisogono (right panel) for all analyzed stations in the EMEP domain in 2001.

ACPD

9, 9597–9645, 2009

Title Page
Abstract
Introduction
Conclusions
References
Tables
Figures
Back
Close
Full Screen / Esc
Printer-friendly Version
Interactive Discussion

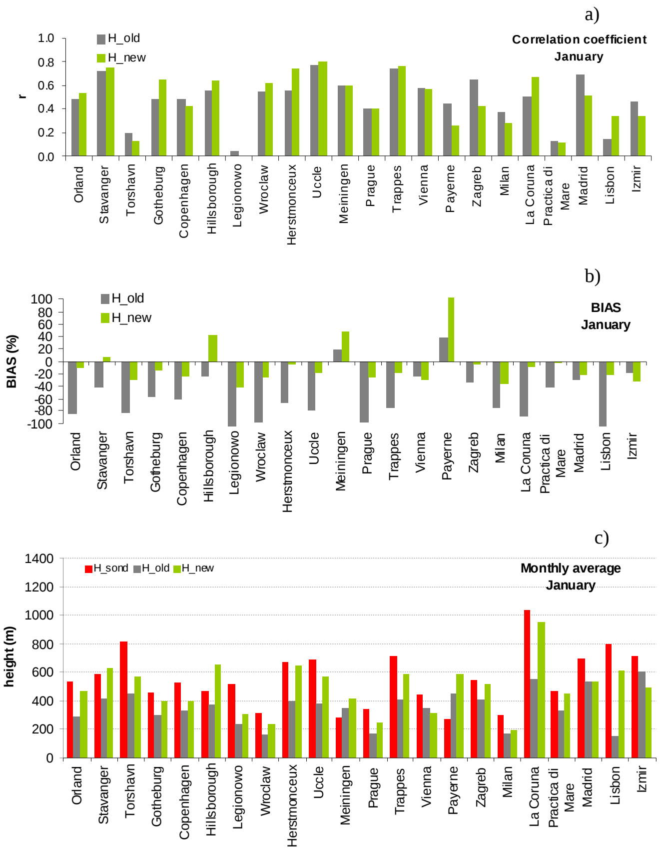

Fig. 11. Monthly: **(a)** r, **(b)** BIAS and **(c)** average calculated between the ABL height, H, determined from the soundings (H_{sond}), and H calculated from the EMEP model with the O'Brien scheme (H_{old}) and with the Ri_B scheme (H_{new}) for different radiosounding station in Europe (Table 1) in January 2001 at 12:00 and 00:00 UTC.

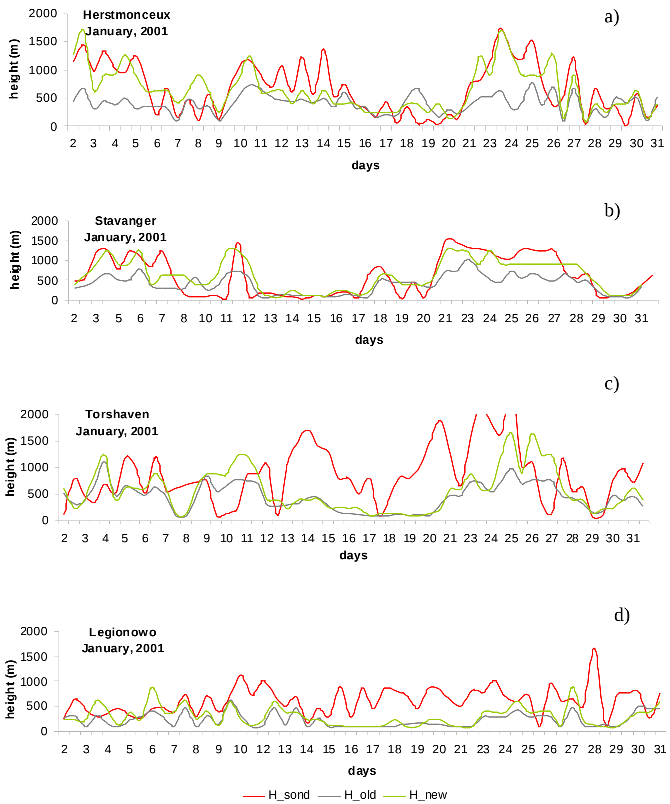

Fig. 12. Time series of H_{sond}, H_{old} and H_{new} at **(a)** Herstmonceux, **(b)** Stavanger, **(c)** Torshavn and **(d)** Legionowo in January 2001.

ACPD

9, 9597–9645, 2009

Title Page
Abstract
Introduction
Conclusions
References
Tables
Figures
◂◂ ▸▸
◂ ▸
Back
Close
Full Screen / Esc
Printer-friendly Version
Interactive Discussion

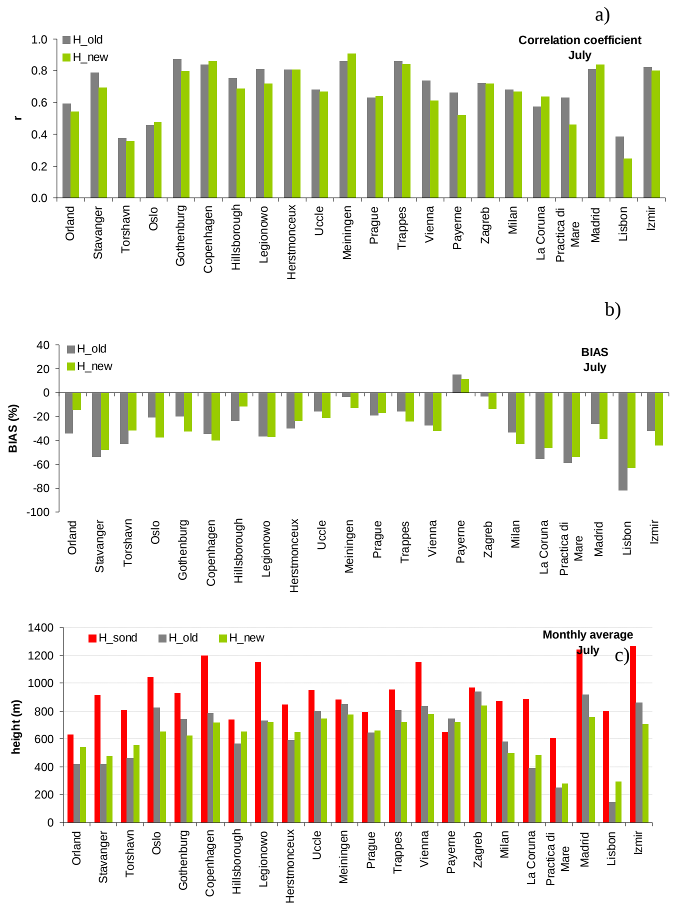

Fig. 13. Same as Fig. 11 but for July, 2001 at 12:00 and 00:00 UTC.

ACPD
9, 9597–9645, 2009

Parameterization of vertical diffusion

A. Jeričević et al.

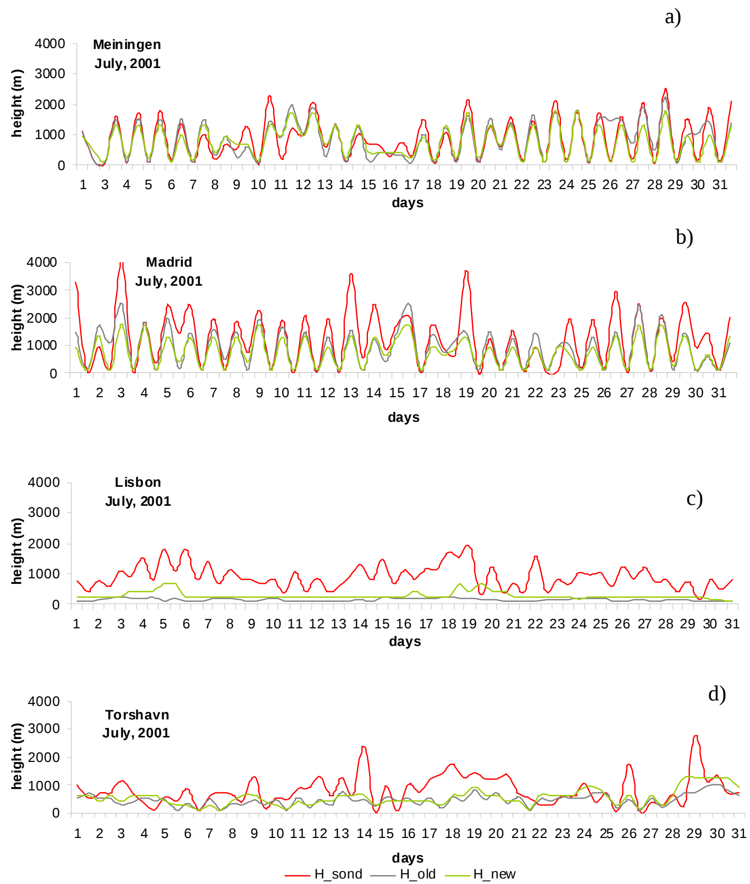

Fig. 14. Same as Fig. 12 but for **(a)** Meiningen, **(b)** Madrid, **(c)** Torshavn and **(d)** Lisbon in July 2001.

ACPD
9, 9597–9645, 2009

Title Page
Abstract | Introduction
Conclusions | References
Tables | Figures
◀I | ▶I
◀ | ▶
Back | Close
Full Screen / Esc
Printer-friendly Version
Interactive Discussion

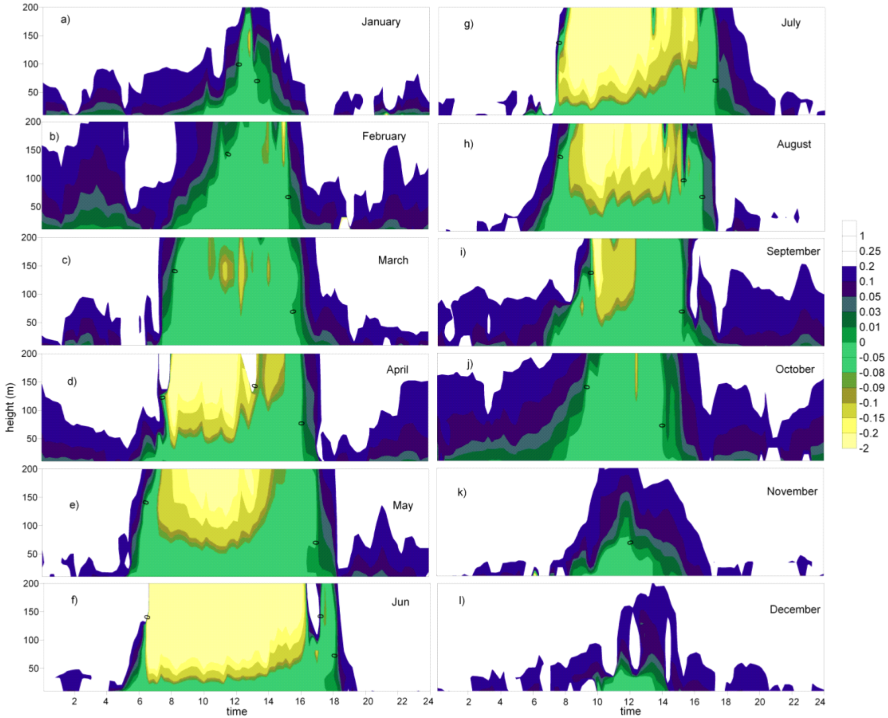

Fig. 15. Monthly vertical profiles of average hourly Ri_B number calculated from the Cabauw data in from January **(a)** to December (l) in year 2001. The ABL height, H, is represented with Ri_{BC}=0.25 (the top of the blue area).

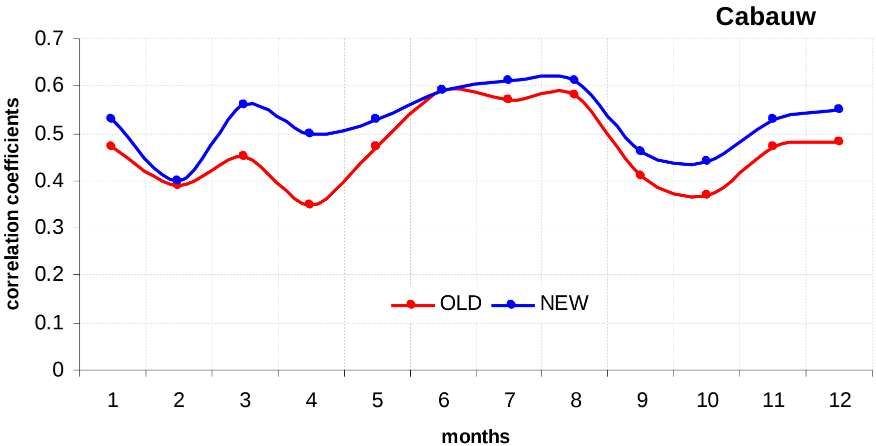

Fig. 16. Monthly r between the H calculated from the Cabauw measurements, and the H calculated with the old (H_{old}) – red, and the new ABL scheme (H_{new}) – blue, in the EMEP model for year 2001.

ACPD
9, 9597–9645, 2009